Journal Pre-proofs

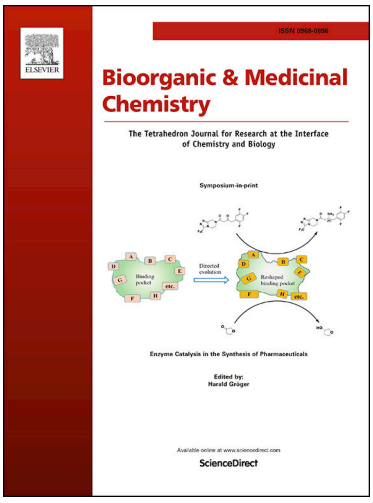

Antibody drug conjugates of cleavable amino-benzoyl-maytansinoids

Thomas Nittoli, Frank Delfino, Marcus Kelly, Serena Carosso, Thomas Markotan, Arthur Kunz, Zhaoyuan Chen, Shu Mao, Jing Shan, Elizabeth Navarro, Feng Zhao, Sosina Makonnen, Carlos Hickey, Jan Spink, William Olson, Jessica R. Kirshner, Gavin Thurston, Nicholas Papadopoulos

PII: S0968-0896(20)30615-5
DOI: https://doi.org/10.1016/j.bmc.2020.115785
Reference: BMC 115785

To appear in: *Bioorganic & Medicinal Chemistry*

Received Date: 16 August 2020
Revised Date: 9 September 2020
Accepted Date: 18 September 2020

Please cite this article as: T. Nittoli, F. Delfino, M. Kelly, S. Carosso, T. Markotan, A. Kunz, Z. Chen, S. Mao, J. Shan, E. Navarro, F. Zhao, S. Makonnen, C. Hickey, J. Spink, W. Olson, J.R. Kirshner, G. Thurston, N. Papadopoulos, Antibody drug conjugates of cleavable amino-benzoyl-maytansinoids, *Bioorganic & Medicinal Chemistry* (2020), doi: https://doi.org/10.1016/j.bmc.2020.115785

Graphical Abstract

To create your abstract, type over the instructions in the template box below.
Fonts or abstract dimensions should not be changed or altered.

Antibody drug conjugates of cleavable amino-benzoyl-maytansinoids

Leave this area blank for abstract info.

Thomas Nittoli[a],* Frank Delfino [a], Marcus Kelly [a], Serena Carosso [b], Thomas Markotan [b], Arthur Kunz [a], Zhaoyuan Chen [a], Shu Mao [a], Jing Shan [a], Elizabeth Navarro [a], Feng Zhao [a], Sosina Makonnen [a], Carlos Hickey [a], Jan Spink [b], William Olson [a], Jessica R. Kirshner [a], Gavin Thurston [a], and Nicholas Papadopoulos [a]

[a]*Regeneron Pharmaceuticals, Inc., 777 Old Saw Mill River Road, Tarrytown, New York 10591*
[b]*Abzena, 360 George Patterson Blvd, Bristol, PA 19007*

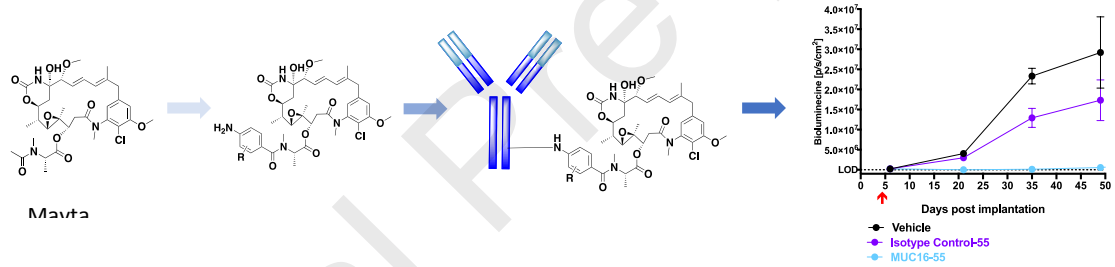

ELSEVIER

Bioorganic & Medicinal Chemistry
journal homepage: www.elsevier.com

Antibody drug conjugates of cleavable amino-benzoyl-maytansinoids

Thomas Nittoli[a],* Frank Delfino[a], Marcus Kelly[a], Serena Carosso[b], Thomas Markotan[b], Arthur Kunz[a], Zhaoyuan Chen[a], Shu Mao[a], Jing Shan[a], Elizabeth Navarro[a], Feng Zhao[a], Sosina Makonnen[a], Carlos Hickey[a], Jan Spink[b], William Olson[a], Jessica R. Kirshner[a], Gavin Thurston[a], and Nicholas Papadopoulos[a]

[a]*Regeneron Pharmaceuticals, Inc., 777 Old Saw Mill River Road, Tarrytown, New York 10591*
[b]*Abzena, 360 George Patterson Blvd, Bristol, PA 19007*

ARTICLE INFO

Article history:
Received
Received in revised form
Accepted
Available online

Keywords:
Antibody
Antibody drug conjugate
Maytansinoid
MUC16

ABSTRACT

ADCs based on the natural product maytansine have been successfully employed clinically. In a previous report, ADCs based on hydrophilic non-cell permeable maytansinoids was presented. The authors in this report further explore the maytansine scaffold to develop tubulin inhibitors capable of cell permeation. The research resulted in amino-benzoyl-maytansinoid payloads that were further elaborated with linkers for conjugating to antibodies. This approach was applied to MUC16 tumor targeting antibodies for ovarian cancers. A positive control ADC was evaluated alongside the amino-benzoyl-maytansinoid ADC and the efficacy observed was equivalent while the isotype control ADCs had no effect.

* Corresponding author. Tel.: 914-847-5420; fax: 914-847-1665; e-mail: thomas.nittoli@regeneron.com

1. I

To continue our research into the microtubule inhibitor Maytansine (**1**), an ansa macrolide first reported by Kupchan in 1972, we explored additional analogs.[1] We first reported on the charged and hydrophilic derivatives of maytansine used as payloads for antibody drug conjugates (ADCs) that were efficacious in pre-clinical models of EGFRvIII expressing tumors (Glioblastoma Multiforme) that were cell impermeable.[2] In that article we reported that our efforts to develop a cell permeable payload were unsuccessful. However, with a different approach we designed payloads that were not charged and were hydrophobic to complement our success with cell impermeable payload ADCs.

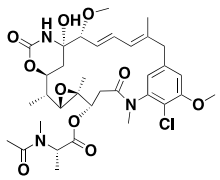

1

Figure 1. Structure of maytansine.

In this report, we continue to expand on the potential utility of the anti-cancer natural product maytansine. Synthesizing a number of amino-benzoyl-maytansinoids containing payloads and assessing their utility for linker attachment we found chemistries suitable for attaching the linker payload to the antibody. Our goal was to increase the cytotoxic effects through cell penetration ("bystander effect"[3]) and by using enzymatically cleavable linker assemblies[4,5], a promising ADC that demonstrated outstanding efficacy against MUC16, an ovarian cancer antigen, expressing tumor xenografts was developed.

2. Results and Discussion

2.1 Synthesis of Payloads and Linker-Payloads

Since we experienced biologically active compounds previously, modifications to the core macrocycle were investigated by substitution at the *N*-methyl alanine nitrogen. This time we kept the length short and hydrophobic by using benzoyl groups. An amino group was postulated to provide an uncharged handle to which a linker could be attached. These amino-benzoyl-maytansinoids were synthesized from des-acetyl-maytansine[6] and the corresponding nitro benzoic acids (Scheme 1). Compounds **19** thru **34** were synthesized in two steps. The nitro benzoic acids were coupled to des-acetyl-maytansine (**18**) using HATU and the nitro group reduced using zinc powder under acidic conditions.

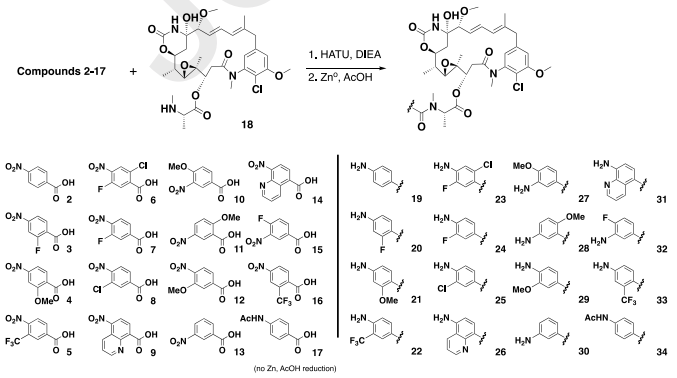

Of the payloads listed above, 4 were selected (**19, 20, 29** and **33**), based on activity *in vitro* cytotoxicity assays (*vide infra*) and solubility, for attachment to linkers suitable for antibody conjugation. The synthetic route to these linker-payload combinations are described below (Scheme 2).

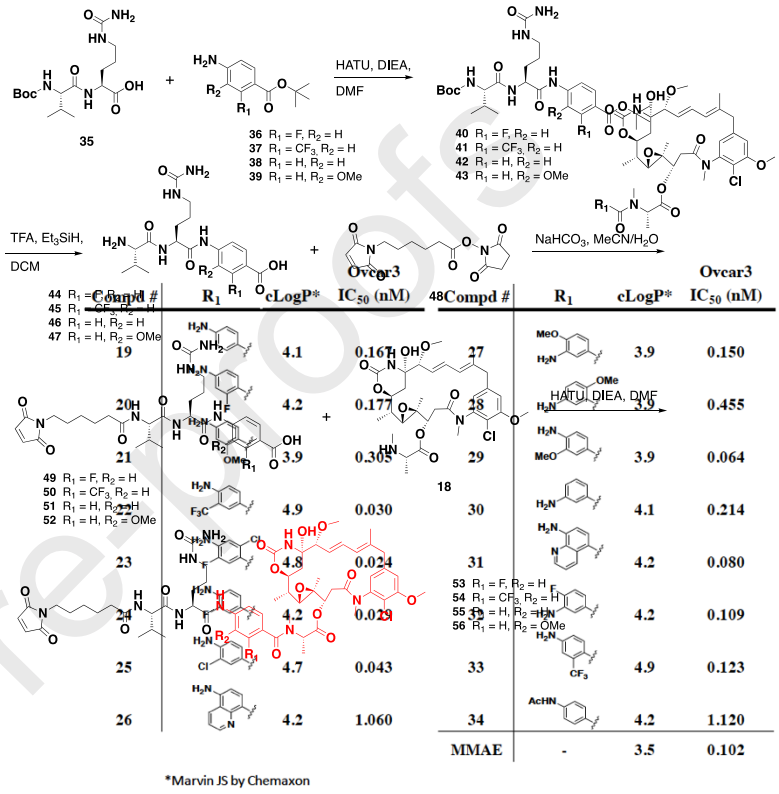

Compd #	R_1	cLogP*	Ovcar3 IC_{50} (nM)
19		4.1	0.167
20		4.2	0.177
21		3.9	0.305
22		4.9	0.030
23		4.8	0.024
24		4.2	0.029
25		4.7	0.043
26		4.2	1.060
27		3.9	0.150
28		3.9	0.455
29		3.9	0.064
30		4.1	0.214
31		4.2	0.080
32		4.2	0.109
33		4.9	0.123
34		4.2	1.120
MMAE	-	3.5	0.102

Scheme 2. Synthesis of linker payloads **53-56**.

The linker-payloads **53** thru **56** were synthesized in four steps. Starting from the Boc-valine-citrulline dipeptide **35**, a HATU coupling with known *t*-butyl ester protected 4-amino benzoates furnished **36** thru **39**. Removal of the ester followed by coupling with the active NHS ester **48** gave the maleimido dipeptide benzoic acids **49** thru **52**. Another HATU coupling provided the final linker payloads **53** thru **56**.

A non-cleavable linker payload was synthesized by HATU coupling of **48** with **19** to yield **57** (Scheme 3).

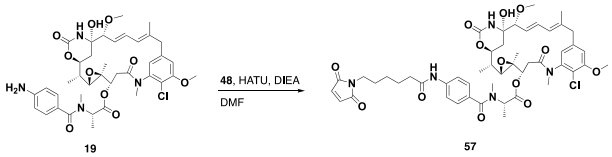

Scheme 3. Synthesis of non-cleavable linker payload **57**.

2.2 *In vitro* Cytotoxicity - Payloads

potency in Ovcar3 (Table 1) and were able to kill these cells almost completely (95 to 100%). With the exception of compounds **26** and **34**, the amino-benzoyl-maytansinoids were comparable or more potent than the clinical standard ADC using the tubulin damaging compound monomethyl aurisatin E (MMAE).[7] All of these amino-benzoyl payloads are also assumed to be devoid of any appreciable charge and as such could freely permeate the cell. Generally, the more hydrophobic the amino-benzoyl-maytansinoid payloads (entries **22, 23,** and **25**) were the most potent likely due to increased cell permeability (also likely to possess a "bystander effect"). Compound **33** had a high cLogP at 4.9, but was slightly less potent at 0.123 nM. The more hydrophilic payloads trended to be slightly less potent, compounds **21**, **27**, and **28** (with the exception of **29**). Even so, these maytansinoid analogs possess remarkable cytotoxic ability with

Table 1. Payload *in vitro* cytotoxicity IC_{50}s.

compounds **26** and **34** (~1 nM) being the least potent. Moving an electron donating methoxy group and amino around the ring (compounds **21**, **27**, **28**, and **29**) probed for the optimal positions for activity. The *para*-amino and *meta*-methoxy groups had the greatest potency at 0.064 nM. A similar movement of an electron withdrawing fluorine group and the electron donating amino group also produced a *para*-amino and *meta*-fluoro group substitution pattern that was amongst the most potency compounds (compound **24**, 0.029 nM). This trend continued with the trifluoromethyl group substitution at the *meta* position, compound **22** (0.030 nM) versus the *ortho* position, compound **33** (0.123), a 4 fold difference. Compounds **23** and **25**, which were amongst the highest hydrophobic analogs, also followed the meta substituted pattern (0.024 and 0.043 nM, respectively). The quinoline compounds **26** and **31** had a remarkable potency difference based on the position of the ring nitrogen. A ring nitrogen in the pseudo-*meta* position gave rise to a ~10 fold increase in potency over the pseudo-*ortho* position of the ring nitrogen, compound **31** (0.080 nM) versus **26** (1.06 nM). Lastly, acetylation of the anilino group in **19** decreases activity by ~7 fold.

2.3 *In vitro* enzyme release of payload 19 from 55

Prior to the preparation of ADCs of payloads of interest with the desired targeting antibodies, an *in vitro* assay was developed and performed in order to determine if designed payload **19** could be released from the linker-payload. Thus, cathepsin B (a lysosomal enzyme) was employed for the cleavage of the valine-citrulline *p*-amino-benzamide payload. Released payload **19** with a mass of 791.27 M+Na (calc'd monoisotopic mass for $C_{39}H_{49}ClN_4O_{10}$, 768.31) was detected minutes into the experiment while the control samples without cathepsin B contained the intact linker payload **55** with a mass of 1240.50 M+Na (calc'd monoisotopic mass for $C_{60}H_{80}ClN_9O_{16}$, 1217.54). Proteolysis of **19** should occur after internalization of the ADC in the cell where the enzyme mainly exists. Off target effects should be reduced since the antibody delivers the cytotoxic payload directly to targeted cells.

2.4 *In vitro* cytotoxicity - ADCs

Having the experience of not only synthesizing linker payloads but also conjugating those compounds to antibodies, we selected a representative group of payloads. Payloads **19**, **20**, **29**, and **33**

based upon their hydrophobicity. This was realized once

ADC	DAR	Ovcar3 IC_{50} (nM*)	HEK293 IC_{50} (nM)
3A5-mc-VC-PAB-MMAE	2.2	0.818 (100)	>100
Isotype Control-mc-VC-PAB-MMAE	2.2	59.2 (100)	>100
3A5-55	1.5	1.40 (97)	>100
3A5-56	1.5	1.18 (100)	>100
Cell Surface Expression		~176K copies	na

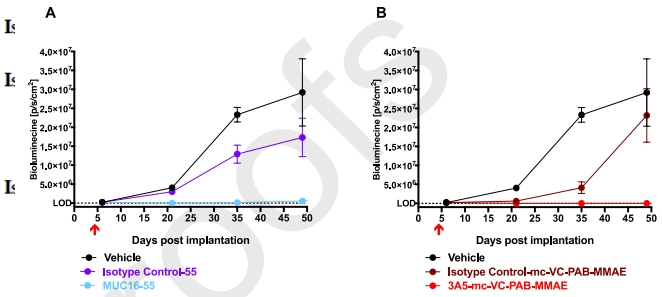

* Values in paratheses are the percent of cell kill

* Values in paratheses are the percent of cell kill

Table 2. ADC *in vitro* cytotoxicity IC_{50}'s.

monomeric ADCs were produced from compounds **55**, **56**, and **57**. Compounds **20** and **33** would represent a more challenging couple of payloads because of their higher cLogP and the implication of aggregate formation once conjugated to an antibody. These two payloads were easier to access the linker payloads synthetically (compounds **53** and **54**, respectively), however produced aggregate once conjugated to the antibodies. It has been shown that site-specifically conjugating challenging linker payloads could help mitigate aggregate formation.[8] That approach could be employed in the future.

The ADCs prepared *via* interchain disulfides by partial reduction of the targeting antibodies and control were assayed against two cell lines (Table 2). Several ovarian cancer targeting ADCs have transitioned to the clinic.[9] Two MUC16 targeting ADCs containing the linker payload mc-VC-PAB-MMAE conjugated randomly to the interchain disulfides (DMUC5754A[10]) or site-specifically to engineered cysteines (DMUC4064A[11]) are among those that have transitioned to the clinic. The positive targeting antibody we employed came from the clinical DMUC5754A, 3A5, and our own MUC16 program.[12] We first assayed our linker payloads conjugated to the positive control antibody, 3A5. The 3A5 ADCs of compounds **55** and **56** were comparable to the clinical control and were more selective since the isotype controls of our ADCs did not kill Ovcar3 cells as did the Isotype Control-mc-VC-PAB-MMAE, IC_{50}= 59.2 nM with 100% cell killing.

Focusing our efforts on cleavable linker payloads **55** and **56**, ADCs from our MUC16 program were conjugated and yielded similar results to the clinical control (IC_{50} = 0.818 vs 0.796 or 0.822 nM, clinical ADC vs ours, respectively). Finally, all of the ADCs produced were assayed against the negative cell line HEK293 and every targeting or isotype control were devoid of activity up to an IC_{50} of 100 nM.

2.5 *In vivo* Efficacy

The MUC16-**55** ADC was studied for efficacy using an *in vitro* cell line for viability assays that could also be grown *in vivo* (Ovcar3 endogeneously expresses the target antigen MUC16). Shown in Figure 2A is the single dose of 5 mg/kg for two ADCs and vehicle, MUC16-**55** and isotype control-**55**, in Ovcar3 tumors. The isotype control lacked efficacy along with vehicle (PBS w/5% glycerol). The targeting MUC16-**55** ADC suppressed tumor growth out to 50 days (Figure 5A). For our comparison, we conjugated the 3A5 mAb, used in the clinical ADC, with mc-VC-PAB-MMAE

Figure 2. *In vivo* efficacy of MUC16 targeting ADCs in the Ovcar3 tumor model. Graph A shows the MUC16-**55** ADC and graph B shows the 3A5-mc-VC-PAB-MMAE ADC dosed at 5 mg/kg (in each study with the exact dosing for control) IV in SCID mice.

randomly to the interchain disulfides (similar to the DMUC5754A ADC) and dosed in the same Ovcar3 *in vivo* model.[13] The 3A5-mc-VC-PAB-MMAE ADC, when dosed once at 5 mg/kg IV, suppressed tumor growth for a similar 50 days, while the vehicle was not effective (Figure 2B). There was efficacy with the isotype control ADC initially, but the tumors recovered by day 50.

The Ovcar3 *in vivo* model was used previously for the 3A5-mc-VC-PAB-MMAE ADC and provides an excellent comparison between the linker payload developed in this study (*vid supra*). The previous preclinical report of 3A5-mc-VC-PAB-MMAE when dosed at 3x2 mg/kg IV displayed similar tumor suppression at 28 days by bioluminescence. It could be speculated that if MUC16-**55** ADC were dosed in a fractionated 3x2 mg/kg IV manor, comparable tumor control would be realized.

3. Conclusion

To continue our quest to further the research on the anti-cancer natural product maytansine, we have developed several novel payloads and linker-payload combinations. Our second goal of developing an ADC with a cell-penetrating payload was realized. These payloads were potent in the *in vitro* Ovcar3 cell line endogenously expressing antigen with 3 payloads possessing 3-4 fold more potency than MMAE. The Muc16 targeting ADC (MUC16-**55**) was able to suppress tumors in the Ovcar3 tumor model with similar efficacy as the clinical positive control **(**3A5-mc-VC-MMAE). It's interesting to point out that the mc-VC-PAB-MMAE linker payload is now used in 3 FDA approved ADCs, Adcetris®, Polivy™, and Padcev™. This work completes our dual goal of producing ADCs with cell impermeable (*vid supra*) and cell permeable maytansinoid payloads ("bystander" capable payloads).

Although we have presented convincing data on an alternative linker payload and antibody delivery vehicle for an ovarian cancer therapeutic, Regeneron had a promising parallel discovery program for a CD3 bispecific. The MUC16xCD3 bispecific antibody (REGN4018) has transitioned into the clinic and we eagerly await results.[14]

4. Experimental Methods

4.1 Synthesis

nds are listed in the supplemental materials.

4.2 *In Vitro* Cytotoxicity

Ovcar3 (MUC16+) and HEK293 (MUC16-) cells were seeded in 96 well plates at 3000 cells per well in complete growth media and grown overnight. For cell viability curves, serially diluted conjugates or payloads were added to the cells at final concentrations ranging from 300 nM to 5 pM and incubated for 8 days. To measure viability, cells were incubated with CCK8 (Dojindo) for the final 1-3 hours and the absorbance at 450nm (OD_{450}) was determined on a Victor (Perkin Elmer). Background OD_{450} levels determined from digitonin (40 nM) treated cells were subtracted from all wells and viability is expressed as a percentage of the untreated controls. IC_{50} values were determined from a four-parameter logistic equation over a 10-point response curve (GraphPad Prism) in quadruplicate. All conjugate curves and IC_{50} values are corrected for payload equivalents.

4.3 Cell Surface Expression

The 3A5 antibody literature measurements were averaged and reported in Table 2.[13]

4.4 Conjugation and Characterization

Three antibodies were conjugated to various linker payload compounds using the procedure below. The targeting antibodies used in these experiments were: (1) an internally generated antibody and (2) an anti-MUC16 antibody from the literature, 3A5. All the monoclonal antibodies were expressed in CHO cells and purified by Protein A. A non-binding isotype control antibody derived from an immunological antigen having no relation to oncology was also used.

The antibody (10 mg/ml) in 50 mM HEPES, 150 mM NaCl, pH 7.5, was treated with 1 mM dithiothreitol at 37 °C for 30 min. After gel filtration (G-25, pH 4.5 sodium acetate), the maleimido linker payload derivatives **55**, **56**, and **57** (1.2 equivalents/SH group of the cysteine residue) in DMSO (10 mg/ml) was added to the reduced antibody and the mixture adjusted to pH 7.0 with 1 M HEPES (pH 7.4). After 1 h the reaction was quenched with excess N-ethyl maleimide. The conjugates were purified by size exclusion chromatography using Dulbecco's PBS with 5% glycerol and sterile filtered. Protein and linker payload concentrations were determined by UV spectral analysis. Size-exclusion HPLC established that all conjugates used were >95% monomeric, and RP-HPLC established that there was <0.5% unconjugated linker payload. All conjugated antibodies were analyzed by UV for linker payload loading values according to Hamblett[15].

4.5 Enzyme cleavage of compound 55

The linker payload **55** was set at 100 µg/mL final in 25 mM sodium acetate buffer, 1 mM EDTA, pH 5.0 and pre-incubated at 37˚C. Cathepsin B (Sigma # C8571) was activated at room temperature for 15 minutes with 1 equivalent of 30 mM DTT, 15 mM EDTA to 2 equivalents of cathepsin B stock. The activated cathepsin B solution was added to the substrate solutions at a 1:20 molar ratio (purified H_2O, instead of activated cathepsin B was added for the control sample.) Samples were incubated at 37˚C

over[illegible]trol through Q1 Scan.

Samples are centrifuged at 12,000 g for 5 min. Supernatant was recovered and analyzed by liquid chromatography-mass spectrometry (Thermo Quantiva) by combined infusion of 0.3 ml/min of 30:70 mobile phase B:A (Mobile Phase A: 0.1% formic acid in H_2O; Mobile Phase B: 0.1% formic acid in Acetonitrile) at 20 µl/min from supernatant. MS1 is set at an appropriate range for detection of molecular ion of either linker payload or payload. The supernatant contained the predicted payload, amino-benzoyl-maytansinoid, with a mass of 791.27 M+Na (calc'd monoisotopic mass for C39H49ClN4O10, 768.31) and the control samples without cathepsin B contained **55** with a mass of 1240.50 M+Na (calc'd monoisotopic mass for C60H80ClN9O16, 1217.54). No predicted payload molecular ion was detected in the control samples.

4.6 *In vivo* Efficacy

Anti-tumor efficacy was assessed in an intraperitoneal tumor model using MUC16 endogenously expressing OVCAR-3 cells [NIH:OVCAR-3 (OVCAR3, ATCC HTB-161)] that were transfected with luciferase (OVCAR3/luc). Tumor cells were serially passaged IP in female SCID mice (Taconic, Hudson NY). For the efficacy study, 1 x 10^6 OVCAR3/luc cells were implanted IP and mice were randomized by luminescent signal on Day 5 post implantation into treatment groups of 8. Animals were then IV dosed 5 mg/kg with either anti-MUC16 drug conjugated reagents, including non-binding ADCs using either **55** or mc-VC-PAB-MMAE linker-payload formats, were dosed at 5 mg/kg. In addition, a PBS with 5% glycerol vehicle was administered and all doses were monitored by detection of the tumor bioluminescence signal, after injection with luciferin, expressed as p/s/cm^2. In these *in vivo* studies, ADCs were dosed and tumors were then monitored until ascites developed in the cohort dosed with vehicle alone. Additional technical details of the *in vivo* model can be found in our MUC16xCD3 bispecific antibody publication.[16]

Acknowledgments

This project was funded by Regeneron Pharmaceuticals, Inc. We gratefully thank the members of the Therapeutic Proteins and Oncology & Angiogenesis groups for all their support. We also thank Steven Maio and Madison Horvath for critical reading of the manuscript and supporting information.

Supplementary data

Experimental procedures for all compounds and intermediates, mass spec, and NMR spectra (PDF) associated with this article can be found in the online version at XXXX.

References and Notes

[1] Kupchan, S. M., Sigel C. W., Guttman, L. J., et al, *J. Am. Chem. Soc.*, 1972;94:1354-1356.
[2] Nittoli, T., Kelly, M., Delfino, F., et al, *BMC*, 2018; 26:2271–2279.
[3] Kovtun, Y. V., Audette, C A., Ye, Y., et al, *Cancer Res.,* 2006;66:3214-3221.
[4] Dubowchik, G. M., Firestone, R. A., Padilla, L., et al, *Bioconjugate Chem.*, 2002;13:855-869.
[5] King, H. D., Dubowchik, G. M., Mastalerz, H., et al, *J. Med. Chem.* 2002;45:4336-4343.
[6] See PCT Int. Appl. (**2016**), WO 2016149464.
[7] Francisco, J. A., Cerveny, C. G., Meyer, D. L., et al, *Blood*, 2003;102;1458-65.
[8] Jeffrey, S. C., Burke, P. J., Lyon, R. P., et al, *Bioconjugate Chem.*, 2013; 24, 7, 1256-1263.
[9] Stewart, D. and Cristea, M., *Curr Opinion Obst. Gyn.* 2019 31 18-23.
[10] Clinical trial NCT01335958
[11] Clinical trial NCT02146313
[12] See PCT Int. Appl. (**2016**), WO 2018058003.
[13] Chen, Y., Clark, S., et al, Cancer Res. 2007 67 4924-4932.
[14] Clinical trial NCT03564340
[15] Hamblett, K. J., Senter, P. D., Chace, D. F., et al, *Clin. Cancer Res.* 2004;10:7063-7070.
[16] Crawford, A., Haber L., Kelly, M. P., et al, *Sci. Transl. Med.* 2019;11, eaau7534 .